LUBRICATION AND CONTAMINATION
effects on bearing life

Bearing life is influenced by many factors. Two of the most important are lubrication and contamination. Through a better understanding of the mechanisms that lead to reduced bearing life owing to the effects of such factors, we can improve bearing design and operation. In this two-part series of articles we focus firstly on lubrication.

The use of rolling bearings in machines provides the clear advantage of reducing friction losses and increasing the overall efficiency of the system. This can be achieved only if the risk of fatigue failure is sufficiently reduced. Rolling bearings, however, exploit the concentrated nature of rolling contacts (Hertzian contacts) to carry the load; this produces high localized pressures and stresses and, therefore, needs good lubrication quality and surfaces to avoid further stress concentrations.

Surface roughness, particle denting and contamination marks found on bearing raceways can induce stress concentrations and facilitate surface-initiated fatigue. The lubricant film developed at the dent and related local surface stresses are also significant to the crack initiation mechanisms. In this article, a novel methodology is presented to link the micro elastohydrodynamic lubrication film (micro-EHL) and related local stresses to the fatigue life of rolling bearings, i.e. [1]. The applied methodology is based on Fourier analysis of the harmonic components of the surface microgeometry (including indentations) to predict hydrodynamic pressures, stress and induced lubricant film. The application of this method to actual bearing surfaces is discussed and analyzed in relation to some existing micro-contact EHL solutions. Finally, the link is made to the lubrication quality factor η_b used in the life rating of rolling bearings. In the second part of this article the problem of contamination and surface indentation and its relation to the micro-EHL model described here will be addressed.

1. MICRO-GEOMETRY EFFECTS IN BEARING-LIFE RATINGS

Following Ioannides et al. [2], the equation for the calculation of the rolling bearing life reads:

$$L_{10m} = a_{skf}\left(\frac{C}{P}\right)^{p} \qquad (1)$$

In (1) the stress-life modification factor a_{skf}, as defined in [2], has the following form:

$$a_{skf} = \frac{1}{10}\left\langle 1 - \left(\eta\frac{P_u}{P}\right)^{w}\right\rangle^{-c/e} \qquad (2)$$

The penalty factor $0 \le \eta \le 1$ used in a_{skf} gives an average account for the actual stress status of the rolling contact in addition to the idealized smooth Hertzian stress. For an analytical rating of the η factor, it is required to quantify the real stress condition developed in the rolling contact during bearing operation. The actual stress state of the rolling contact may be the result of many surface-induced interactions from local macro and micro surface features. This, in turn, can be related to the amount of surface separation, i.e., lubrication conditions, and particle contamination of the contact. Following [3] a simple rating parameter of the lubrication condition of the bearing is the viscosity ratio κ. Detailed explanations about the derivation of this engineering lubrication parameter can be found in [4]. The κ parameter is defined as the ratio between the actual lubricant viscosity at the operating temperature of the bearing (ν) and a standardized reference viscosity (ν_1) rated as adequate [5, 6] for the lubrication of the bearing. According to [6], the lubrication parameter κ can also be related to the well-known specific film thickness Λ of a rolling contact using the approximation: $\kappa \approx \Lambda^{1.3}$.

Following [2], the penalty factor $0 \le \eta \le 1$

used in (2) can be described as a product of two concurrent quantities, the lubrication factor η_b and the contamination factor η_c as:

$$\eta(\beta_{cc}, d_m, \kappa) = \Psi_{brg} \cdot \eta_b(\kappa)_{nom} \cdot \eta_c(\beta_{cc}, d_m, \kappa) = \eta_b(\kappa)_{brg} \cdot \eta_c(\beta_{cc}, d_m, \kappa) \quad (3)$$

The focus of the present work is the quantification of the surface and subsurface stress conditions (with the inclusion of the EHL lubricant film) associated with the above parameters (3) to provide an analytical measure of the penalty factor η used in bearing dynamic ratings.

Surface stresses induced by geometrical features such as dents, asperities or other imperfections, while passing through the Hertzian contact, have been studied by many authors using analytical, semi-analytical and numerical methods. An early full numerical solution of the EHL contact problem with the inclusion of simple dents or bumps passing through the rolling contact is given in [7].

More recently, a fast technique, based on the use of FFT (Fast Fourier Transform) for the calculation of the EHL pressures and related subsurface stress originated from micro-geometry features such as roughness or dents, has been developed [8, 9]. This methodology is particularly suited to account for the development of the lubricant film and related EHL effects, using real roughness and dent features. This method has provided a new, powerful tool to tackle the micro-EHL problems and related subsurface stresses of real bearing contacts.

In this new scheme, the micro-EHL behaviour of a single sinusoidal roughness wave (or of an assembly of many) is described. By applying the above methodology, the elastic deformation and related pressure waves can be calculated under full transient conditions. The solution for a single sinusoidal roughness and resulting deformed shape and pressures inside the Hertzian contact can then be applied (thus exploiting the fact that in the high-pressures zone the Reynolds Equation can be reduced to a linear form). Fourier analysis can also be applied to the full range of wave frequencies forming the micro-geometrical shape of the raceway. Note that a different technique, also based on Fourier analysis, can be applied to calculate subsurface stresses [9]. The combined use of these numerical techniques for surface and subsurface stresses calculations provides a fast and powerful tool for the analysis of real bearing surface topography. As a result, actual rolling bearing raceways can be evaluated regarding their surface and subsurface stresses under different lubrication conditions.

2. THE MICRO-GEOMETRY PRESSURE AND STRESS MODEL

Traditionally, numerical solutions have been used to model elastohydrodynamic lubrication (EHL) and micro-EHL (accounting for the micro-geometry), thus the Reynolds equation for the fluid is solved iteratively with the elasticity equation for the steel and the lubricant state equations (piezo-viscosity and compressibility), e.g. [10]. Micro-geometry and roughness in one of the surfaces means time-dependent effects in the solution due to the influence of the squeeze effects in the Reynolds equation, which for a line contact is

$$\frac{\partial}{\partial x}\left(\frac{\rho h^3}{12\hat{\eta}}\frac{\partial p}{\partial x}\right) = \bar{u}\frac{\partial(\rho h)}{\partial x} + \frac{\partial(\rho h)}{\partial t} \quad (4)$$

where ρ is the local lubricant density, p is the local pressure, h is the local film thickness, $\hat{\eta}$ is the local viscosity and x, y are space coordinates (x along rolling direction), t is the time and $\bar{u}$ is the entrainment lubricant speed in the contact.

The analysis follows [8]. In an EHL contact, the pressures are so high that the lubricant becomes nearly solid, thus $\hat{\eta} \to \infty$ and the Reynolds equation can be linearized:

$$\frac{\partial(\rho h)}{\partial x} + \frac{\partial(\rho h)}{\partial t} = 0 \quad (5)$$

This equation can be applied to a low-amplitude single sinusoidal roughness entering into the EHL contact during pure rolling. In this case, the equations behave as a wave-transport equation and an analytical solution for local pressures and film thickness can be found, e.g. [11, 8]. More importantly, since this equation is linear, the powerful Fourier techniques (FFT, IFFT) can be applied to solve complex surface geometries. In this way, micro-EHL pressures and deformed shape can be found for roughness samples at the centre of the Hertzian contact.

Once the EHL pressures are obtained, the subsurface stresses can be calculated. The stresses act upon linear elastic materials (steel), so a technique also based on the Fourier method is used, as described in [9]. Again, all stress components can be calculated for a sinusoidal pressure and associated surface tractions from Coulomb friction. Therefore, the method applied is to calculate all stress components for every pressure and traction sinusoidal component and then reassemble the complete stress field.

2.1. RESULTS FROM MICRO-EHL ANALYSIS

An example is taken where an idealized dent (sinusoidal shape with no shoulders) is modelled while passing through an EHL contact. The contact and lubrication conditions are typical of rolling bearings.

For these conditions and the dent geometry as described in Fig. 1 (but without shoulders) a maximum von Mises stress of 0.34 p_o was obtained. A simulation based on the present FFT approach was carried out, using the same conditions, but with more realistic dent geometry, i.e. dents with shoulder height of 0.15 μm all around the dent (as in elastic-plastic indentation from particles). Since the present technique deals only with pressure and clearance fluctuations, the smooth EHL pressure is approximated to a Hertzian pressure distribution, and it is added. Fig. 1 shows the resulting calculated dimensionless pressures (normalized with respect to the maximum Hertzian pressure) and the clearances (normalized with respect to the central smooth film thickness) when

the dent is at the centre of the contact.

Fig. 2 shows the von Mises stress fields (normalized with respect to the maximum Hertzian pressure) in two planes (at y=0 and x=0) in the centre of the contact corresponding to the distribution of pressures shown in fig. 1. The maximum von Mises stress calculated for this case is 0.42 p_o, which is increased (23 %) from the one given without shoulders, due to the presence of a realistic shoulder height at the edge of the dent.

2.2. APPLICATION OF MICRO-EHL ANALYSIS TO BEARING SURFACE ROUGHNESS

The present micro-EHL model can also be applied to a real bearing surface roughness. In the next section is shown the schematic process of 3D mapping of the bearing raceway topography using an optical profiler. Typical examples of results obtained from the micro-EHL analysis are shown in fig. 3.

In fig. 3a, a sample of the bearing topography is used together with the operating conditions of the lubricated contact for the calculations of the elastically deformed topography (fig. 3b) and related micro-EHL pressure fluctuations (fig. 3c). The associated von Mises subsurface stress field in the rolling direction is shown in fig. 4. Clearly displayed are the micro subsurface stress concentrations induced by roughness micro-contacts.

A second illustrative example (related to a different film thickness) is shown in fig. 5. In this case, an increase of 30 % of the maximum pressure is obtained from a reduction of oil film thickness of about 34 %.

It can be seen with the use of the present methodology that a thinner lubricant film (low κ) tends to produce pressure fluctuations that become more and more similar to the ones obtained using the dry contact condition. A thicker oil film will instead significantly damp the development of pressure fluctuations, leading to a reduced stress condition for the asperities and a lower micro-contact fatigue for the raceway.

In the next section the micro-EHL model will be applied to assess the effect of roughness and lubrication in bearing life.

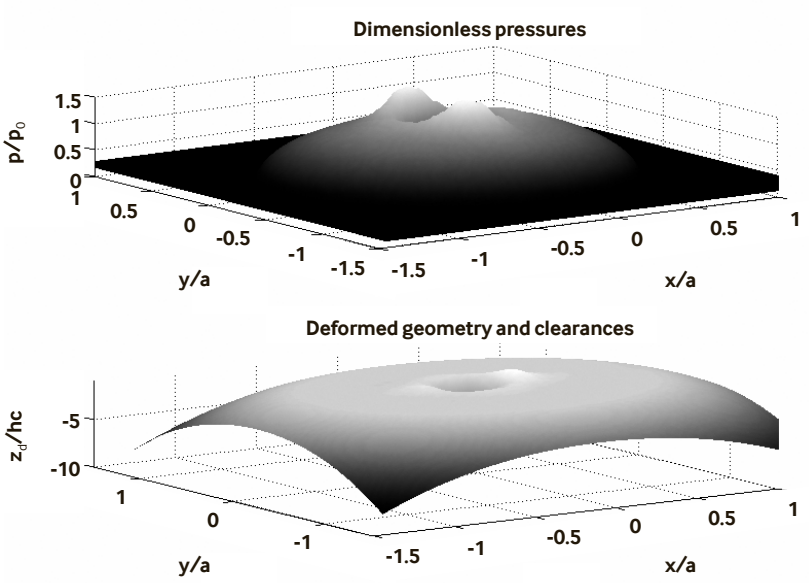

Fig. 1: Normalized pressures and clearances as calculated with the present technique for the dent example and a dent geometry including dent-shoulder height of 0.15 µm. Pure rolling conditions when the dent is at the centre of the contact.

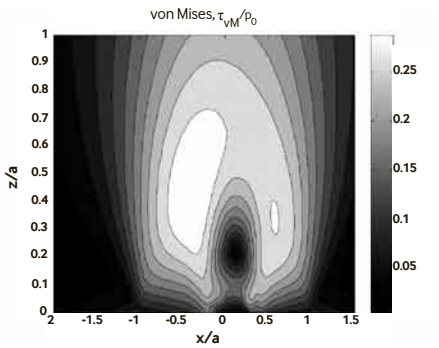

Fig. 2a: von Mises stresses at the centre of the contact for y=0.

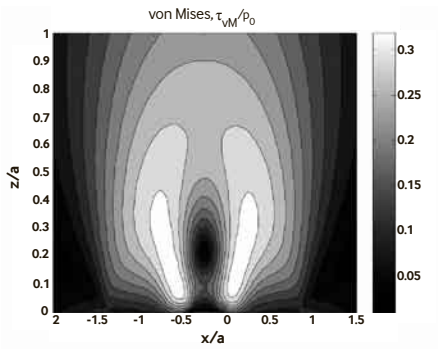

Fig. 2b: von Mises stresses at the centre of the contact for x=0.

Fig. 2: Normalized von Mises subsurface stress distribution for the x and y planes at the centre of the contact. Contact pressure distribution corresponding to Fig. 1.

3. CONNECTION WITH THE LUBRICATION QUALITY FACTOR

The theoretical relationship between the lubrication quality, characterized by the viscosity ratio κ, and the corresponding reduction to the life and fatigue load limit of the bearing will be discussed hereafter. For this purpose one needs to quantify the fatigue life reduction resulting from an actual rolling bearing, with standard surface roughness, compared to the one characterized by an ideally smooth raceway, as from a purely Hertzian, friction-free, stress distribution hypothesis. This can be performed by comparing the theoretical fatigue life between a real bearing (with standard roughness) and the fatigue life of a hypothetical bearing with ideally smooth and friction-free surfaces. Thus, the following life ratio has to be quantified:

$$\frac{L_{10,r}}{L_{10,s}} = \frac{a_{skf,rough}}{a_{skf,smooth}} \qquad (6)$$

The above ratio can be evaluated numerically using the fatigue life stress integral applied to an actual rolling contact [12].

$$\ln\frac{1}{S} \approx A \cdot N^e \int_{V_R} \frac{\langle \tau_i - \tau_u \rangle^c}{z^h}\, dv \qquad (7)$$

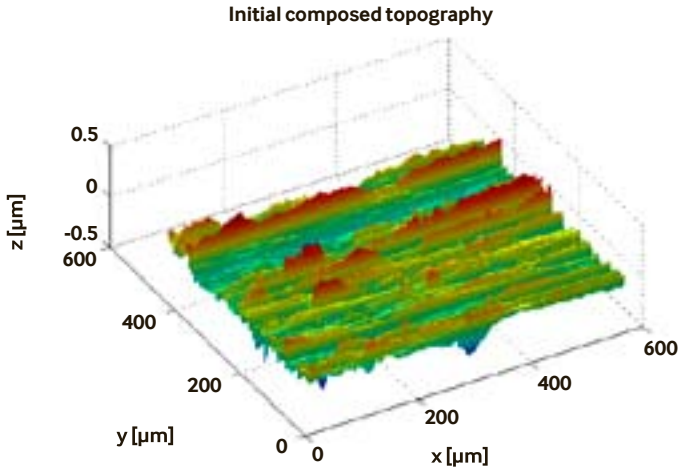

Fig. 3a: Typical initial undeformed gap topography used in the present analysis. (Original roughness: Rq=0.0656 µm).

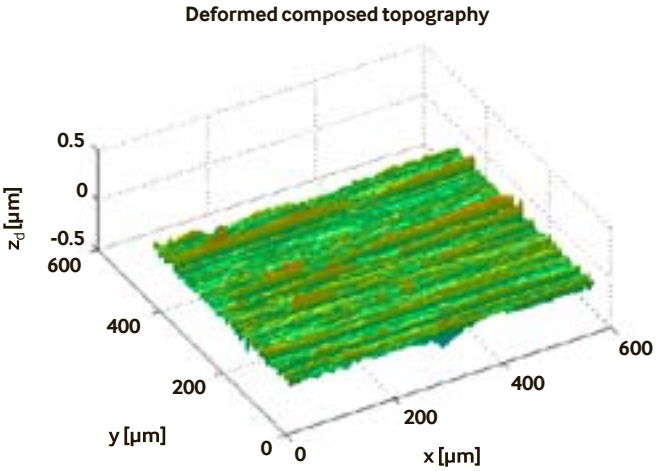

Fig. 3b : Resulting deformed gap topography during the over-rolling of the contact. (Hertzian pressure of the rolling contact 2.17 GPa, central film thickness 0.103 µm).

In equation (7), the relevant quantity affecting the life ratio (6) is the volume-related stress integral, which reads:

$$I = \int_{V_R} \frac{\langle \tau_i - \tau_u \rangle^c}{z^h} \, dv \qquad (8)$$

Using the above notation, the life equation (1) can now be expressed as:

$$L_{10} = \frac{N}{10^6 \, u} \approx \frac{1}{u} \cdot \left(\frac{\ln(1/S)}{A \cdot I} \right)^{1/e} \qquad (9)$$

In this equation, the stress integral (I) can be computed for both standard roughness and for an ideally smooth contact; thus, it can be used for the estimation of the expected effect on the bearing life as given by the life ratio of equation (6). In other words, the following applies:

$$\left(\frac{L_{10,r}}{L_{10,s}} \right)_{(m,n)} = \left(\frac{I_{smooth}}{I_{rough}} \right)^{1/e}_{(m,n)} = \left(\frac{a_{skf,rough}}{a_{skf,smooth}} \right)_{(m,n)} \qquad (10)$$

In general, the ratio (10) depends on the surface topography (index m) and amount of surface separation or amount of interposed lubricant film (index n).

The lubrication factor η_b can now be directly derived from equation (10) by introducing the stress life factor of equation (3). Under the hypothesis of ideally clean lubricant, the contamination factor η_c can be set to unity. Thus, for standard rolling bearing roughness, the stress life factor can be written as:

$$a_{skf,rough} = \frac{1}{10} \left\langle 1 - \left(\eta_b \frac{P_u}{P} \right)^w \right\rangle^{-c/e} \qquad (11)$$

Similarly, in case of a hypothetical bearing with an ideally smooth raceway, the η_b factor can be set to unity and the stress-life factor than becomes:

$$a_{skf,smooth} = \frac{1}{10} \left\langle 1 - \left(\frac{P_u}{P} \right)^w \right\rangle^{-c/e} \qquad (12)$$

Inserting equations (11) and (12) into equation (10) the following is derived:

$$\eta'_{b\,(m,n)} = \frac{P}{P_u} \left\langle 1 - \left\langle 1 - \left(\frac{P_u}{P} \right)^w \right\rangle \cdot \left(\frac{I_{smooth}}{I_{rough}} \right)^{-1/c}_{(m,n)} \right\rangle^{1/w} \qquad (13)$$

Equation (13) shows that a (m x n) matrix of numerically derived η'_b values can be constructed, starting from the calculation of the fatigue life and related stress-volume integral of standard rough bearing surfaces. This calculation must be extended to include different amounts of surface separation (film thickness), from thin films up to full separation of the rolling contact. The calculation procedure illustrated in the next section was applied for the numerical evaluation of the $\eta'_{b(m,n)}$ considering a representative sample of actual rolling bearing surfaces.

Following the methods described above, a set of $\eta'_{b\,(m,n)}$ values was obtained. The resulting data points and interpolation curves are plotted in the κ - η_b diagram shown in fig. 6. For clarity, only a representative group of typical bearing surfaces is presented. The numerically generated curves of $\eta'_b(\kappa)$ consistently show a typical trend with a rapid decline of η'_b for a reduction of the nominal lubrication conditions κ of the contact.

Different authors [10] have discussed

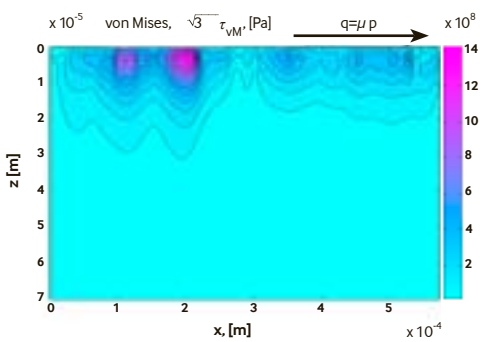

Fig. 4: Subsurface stress field corresponding to the surface pressures shown in fig. 3c; the case considers a friction coefficient µ=0.01, stress distribution at y=0. Hertzian pressure of the contact 2.17 GPa.

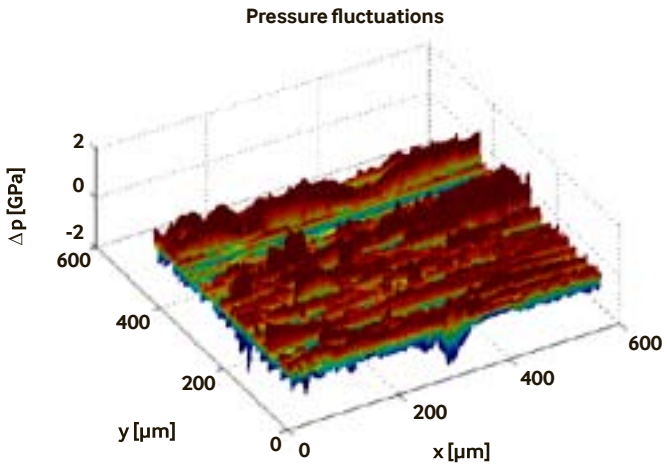

Fig. 3c: FFT calculated pressure fluctuations inside the EHL contact. (Hertzian pressure of the rolling contact 2.17 GPa, central film thickness 0.103 µm).

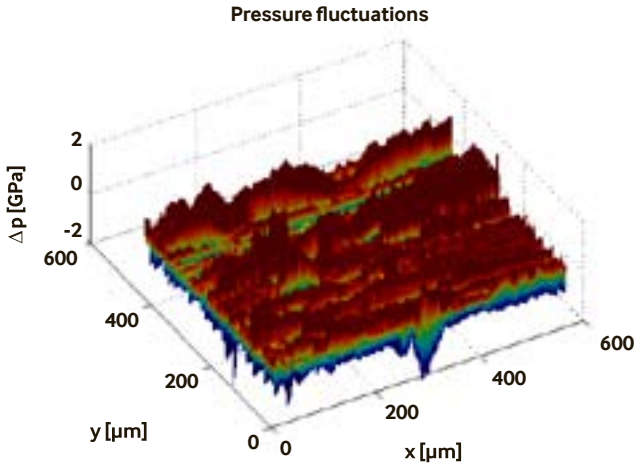

Fig. 5: Pressure fluctuations inside the EHL contact. An increase of 30 % of the maximum pressure is obtained from a reduction of oil film thickness of about 34 %, compared to fig. 3c, all other operating conditions are the same as from the example of fig. 3.

that the dimensionless wavelength parameter $\nabla = (\lambda'/a)\sqrt{M/L}$ would possibly provide a better correlation with the pressure build-up at the asperities and thus with η_b. A lubrication parameter, which would include, in addition to the film thickness, also a measure of the asperities wavelength, would probably provide a better differentiation between the different roughness textures and the corresponding η_b compared to the one shown in fig. 6. However, the requirement of standardized dynamic life ratings is basically to ensure a lower boundary, or safe limit, to the performance of rolling bearings. When used within the range of the many possible types of surface roughness textures, this results in good-quality rolling bearing products. For this purpose, the simple viscosity ratio approach seems sufficient, and indeed convenient, considering that κ is a very well-established lubrication parameter in bearing engineering practice. Regarding the general shape of the $\eta_b(\kappa)$ curves shown in fig. 6, a close resemblance to the life-ratio (Λ) curves obtained by Tallian et al. [3] should be noticed, thus indicating that a single basic physical phenomenon is indeed being observed.

A limitation of the numerical calculations is the requirement of a minimum amount of oil film present in the contact (to preserve continuity condition of the fluid flow equations that are used). Therefore κ values lower than ~ 0.2 couldn't be easily evaluated. Purely dry conditions could also be used to estimate the fatigue stress integral for conditions in which the film can be considered negligible. However, as shown by the general trend of the curves of fig. 6, the tendency of η_b is toward the origin of the diagram for conditions approaching the nominal lower boundary of the κ range.

For comparison, in fig. 6 the lubrication factor equation described in [2] is also shown:

$$\eta_b(\kappa)_{nom} = \eta_b(\kappa)_{brg}/\psi_{brg} = \left(3.387 - \frac{b_1(\kappa)}{\kappa^{b_2(\kappa)}}\right)^{5/2} \quad (14)$$

In (14) the constants b_1 and b_2 are assigned for three intervals of the κ range, and ψ_{brg} is a constant, characterizing each of the four main types of rolling bearings: radial ball, radial roller, thrust ball and thrust roller bearings. In the present assessment we compare the numerically obtained η'_b to the normalized standard form of the lubrication factor $\eta_b(\kappa)_{nom}$ of (14). It is shown that the relationship (14), indicated in fig. 6 with a solid thick line, has a good safety setting compared to the numerically calculated η'_b results. Indeed, fig. 6 shows that nearly all analyzed surface roughness samples are well above the standard limit line. This suggests that equation (14) is a reasonable safe choice for rating the effect of lubrication conditions of the bearing and the expected endurance life.

Some of the roughness textures used in the numerical evaluation belonged to bearings that were also endurance tested. Comparisons between endurance testing lives and lives obtained using the lubrication factor (14) are further discussed in the experimental results (Part 2), which deals with endurance testing of rolling bearing under various lubrication conditions. The overall calculation methodology is then summarized by fig. 7 and described next:

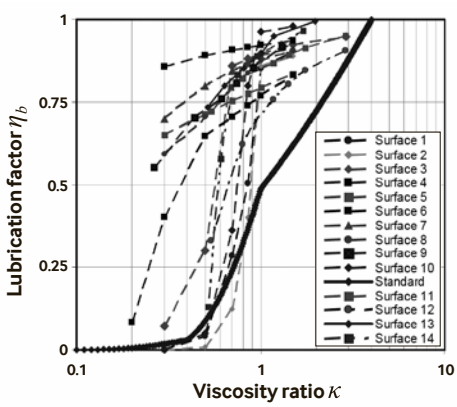

Fig. 6: Summary of numerically calculated lubrication factor for typical surface textures of bearing raceways. Also plotted is the lubrication factor used by bearing standard (thick solid line), as from equation (14), [6].

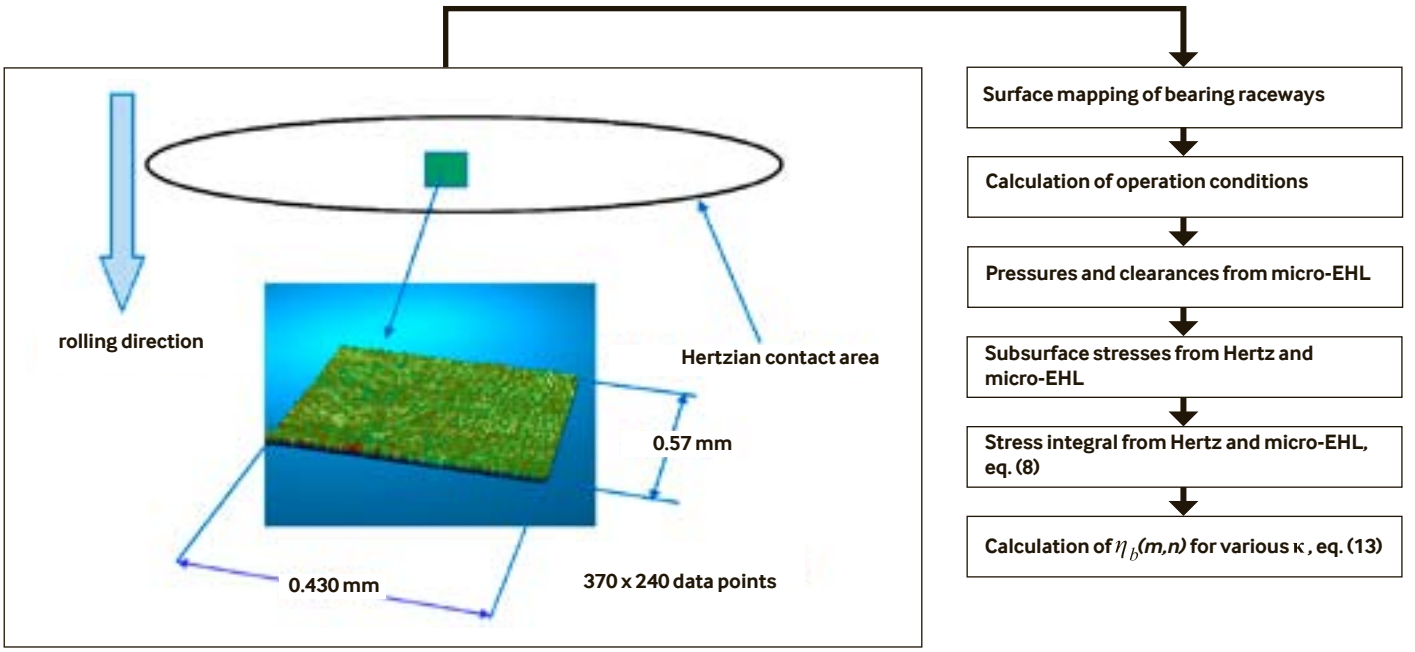

Fig. 7: Schematic representation of surface mapping of the bearing raceway and steps for the calculation of the lubrication factor related to the given specific surface topography and operating conditions.

- Measure real bearing topographies using an optical microscope, representing a spot in the centre of the Hertzian contact.
- Disassemble the measured micro-geometry in sinusoidal components.
- By using the operating conditions in the contact, solve for pressures and deformed shape of every sinusoidal using the analytical solution.
- Reassemble the solution for pressures and film thickness.
- Use the micro-stress methodology to calculate the subsurface stresses.
- Use equation (13) to calculate the η_b parameter for the present case.

4. DISCUSSION AND CONCLUSIONS

The basic theory for deriving the lubrication quality factor in the life rating of rolling bearings has been presented. It is shown that this factor can be related to the calculation of micro-EHL pressures, stresses and fatigue damage, so it represents a measure of the effect of lubrication quality in the life rating of rolling bearings. By using different measured rolling bearing topographies and lubrication conditions, it is shown that different topographies will give different effects in life rating. However, the current $\eta_b(\kappa)$ model as presented in [6] represents a conservative safe limit, which covers well most of the cases analyzed here well.

The micro-EHL methodology presented here represents an efficient method (which avoids the use of computer-intensive numerical solutions) to assess the fatigue damage effect of any low-amplitude topography feature in rolling contacts (roughness or indentations). In the present article (Part 1) the methodology is used to derive the lubrication factor η_b for rolling bearings; in the second part of this article (Part 2) this methodology will be used to derive the contamination factor η_c. ◘

***By** Guillermo Morales Espejel, Antonio Gabelli and Stathis Ioannides, SKF Engineering Research Centre, Nieuwegein, the Netherlands.*

CONCLUSIONS

1. Contrary to current models, the present formulation (at stress level) can fast account for detailed micro-geometry (e.g., surface topography and micro-defects) without performing full EHL numerical simulations. Comparisons with early results (numerical and experimental) indicate good agreement with the present model.

2. It is shown that the lubrication factor in the life of rolling bearings η_b is directly connected to the micro-EHL pressures and stresses present in an EHL contact produced by the surface roughness and quality of lubrication. This factor represents a conservative lower boundary of the calculation of many bearing surfaces.

References

[1] Gabelli, A., Morales-Espejel, G.E., Ioannides, E., *Particle Damage in Hertzian Contacts and Life Ratings of Rolling Bearings,* Tribol. Trans., vol. 51, pp. 428–445, 2008.
[2] Ioannides, E., Bergling, G., Gabelli, A., *An Analytical Formulation for the Life Rating of Rolling Bearings,* Acta Polytechnica Scandinavica, Mech. Eng. Series, 137, 1999.
[3] Tallian, T.E., Chiu, Y.P., van Amerongen, E., *Prediction of Traction and Micro-Geometry Effects on Rolling Contact Fatigue Life,* Trans. ASME, J. of Trib., vol. 100, pp. 156–166, 1978.
[4] Bolton, W.K., *Elastohydrodynamic in Practice,* Rolling Contact Fatigue: Performance Testing of Lubricants, Tourret, R., and Wright, E.P., Ed.; The Institute of Petroleum, London, pp. 17–25, 1977.
[5] Harris, T.A., and Kotzalas, M.N., *Advanced Concepts of Bearing Technology,* CRC Taylor & Francis, 240-246, 2007.
[6] International Standard: *Rolling Bearings – Dynamic load rating and rating life,* ISO 281: 2007.
[7] Venner, C. H., *Mutilevel Solutions of the Line and Point Contact Problems,* Ph.D. dissertation, University of Twente, Enschede, the Netherlands, 1991.
[8] Morales-Espejel, G.E., Lugt, P.M., Van Kuilenburg, J., Tripp, J.H., *Effects of Surface Micro-Geometry on the Pressures and Internal Stresses of Pure Rolling EHL Contacts,* STLE Tribology Transaction Vol. 46, pp. 260-272, 2003.
[9] Tripp, J.H., Van Kuilenburg J., Morales-Espejel G.E., Lugt, P.M., *Frequency Response Functions and Rough Surface Stress Analysis,* STLE Tribology Transaction Vol. 46, pp. 376-382, 2003.
[10] Venner, C.H., and Lubrecht, A.A., *Multi-Level Methods in Lubrication,* Elsevier Science, 2000.
[11] Greenwood, J.A., and Morales-Espejel, G.E., *The Behaviour of Transverse Roughness in EHL Contacts,* Proc. Instn. Mech. Engrs., part J, J. of Eng. Tribo., 208, pp.121-132, 1994.
[12] Ioannides, E., and Harris, T.A., *A New Fatigue Life Model for Rolling Bearings,* Trans. ASME, J. of Trib., 107, pp. 367-378, 1985.